System for $\delta^{13}C$-CO_2 and xCO_2 analysis of discrete gas samples by cavity ring-down spectroscopy

Dane Dickinson[1], Samuel Bodé[2], Pascal Boeckx[2]

[1] Biosystems Engineering, Ghent University, Coupure Links 653, 9000 Gent, Belgium
[2] Isotope Bioscience Laboratory – ISOFYS, Ghent University, Coupure Links 653, 9000 Gent, Belgium

Correspondence to: Dane Dickinson (dane.dickinson@ugent.be)

Abstract. A method was devised for analysing small discrete gas samples (50 ml syringe) by cavity ring-down spectroscopy (CRDS). Measurements were accomplished by inletting 50 ml syringed samples into an isotopic-CO_2 CRDS analyser (Picarro G2131-i) between baseline readings of a standard reference air, which produced sharp peaks in the CRDS data feed. A custom software script was developed to manage the measurement process and aggregate sample data in real-time. The method was successfully tested with CO_2 mole fractions (xCO_2) ranging from <0.1 to >20000 ppm and $\delta^{13}C$-CO_2 values from -100 up to +30000 ‰ vs VPDB. Throughput was typically 10 samples h^{-1}, with 13 h^{-1} possible under ideal conditions. The measurement failure rate in routine use was ca. 1 %. Calibration to correct for memory effects was performed with gravimetric gas standards ranging from 0.05 to 2109 ppm xCO_2 and $\delta^{13}C$-CO_2 levels varying from -27.3 to +21740 ‰. Repeatability tests demonstrated that method precision for 50 ml samples was ca. 0.05 % in xCO_2 and 0.15 ‰ in $\delta^{13}C$-CO_2 for CO_2 compositions from 300 to 2000 ppm with natural abundance ^{13}C. Long-term method consistency was tested over a 9-month period, with results showing no systematic measurement drift over time. Standardised analysis of discrete gas samples expands the scope of applications for isotopic-CO_2 CRDS and enhances its potential for replacing conventional isotope ratio measurement techniques. Our method involves minimal set-up costs and can be readily implemented in Picarro G2131-i and G2201-i analysers or tailored for use with other CRDS instruments and trace gases.

1 Introduction

Cavity Ring-Down Spectroscopy (CRDS) is a high-sensitivity laser absorption technology becoming increasingly common for trace gas analysis (Wang et al., 2008). As well as returning high-resolution mole fraction measurements (Crosson, 2008), CRDS is used for stable isotope analysis of CO_2, CH_4, H_2O, and N_2O (Crosson et al., 2002; Dahnke et al., 2001; Kerstel et al., 2006; Sigrist et al., 2008). Commercial deployment of CRDS has created novel analytical possibilities with greater stability, precision, instrument portability, and a lower cost-basis compared with many traditional spectroscopic, chromatographic, and mass spectrometric techniques (Berryman et al., 2011; Hancock and Orr-Ewing, 2010; Mürtz and Hering, 2010; Picarro, 2009).

Crosson et al. (2002) provide a description of the working principles for making isotopic measurements by CRDS. Commonly used in atmospheric research, isotopic CRDS gas analysers are normally on-line instruments whereby sample gas is continuously pumped through an optical cavity. While such continuous measurement systems are useful for monitoring applications, technical adaption is necessary for routine handling of small discrete gas samples. Commercial add-on modules are available for this purpose (McAlexander et al., 2010; Picarro, 2013), but these are unable to match the rapidity of conventional methods like gas chromatography (GC) and isotope ratio mass spectrometry (IRMS).

CRDS analysis with discrete sample throughput and handling comparable to IRMS could significantly improve a variety of empirical research. For example, simultaneous high-precision isotope ratio and mole fraction measurements from isotopic-CO_2 CRDS will reduce empirical workload and increase accuracy of CO_2 flux partitioning calculations in soil and plant respiration experiments (Midwood and Millard, 2011; Snell et al., 2014). However, realising these benefits requires regular batch analysis of discrete samples – existing arrangements that couple CRDS instruments directly to soil headspace chambers are generally constrained to measuring just one experiment at a time (Albanito et al., 2012; Bai et al., 2011; Midwood et al., 2008).

Berryman et al. (2011) describe a syringe sample delivery system for isotope ratio CRDS that allows small air samples (20 to 30 ml) to be analysed. In their method, the optical cavity of the CRDS analyser is flushed and completely evacuated prior to direct sample injection to ensure consistency and prevent sample-to-sample contamination. Although an important technical innovation with handling and cost advantages over IRMS, the set-up is limited by slow sample turnover rates (3 h^{-1}).

In this paper, we present a new method for measuring discrete syringed gas samples (50 ml) by CRDS. Like Berryman et al. (2011), this method was conceived for isotopic-CO_2 CRDS to provide $\delta^{13}C$-CO_2 and CO_2 mole fraction (xCO_2) analysis in soil respiration studies, but remains general enough to be used in other contexts and adjusted for other gas species. Instead of evacuating the cavity prior to sample introduction, our process intersperses samples against background measurements of a fixed reference air and post-corrects for bias in the measurements. This results in considerably faster throughput for atmospheric samples (up to 13 h^{-1}) than the method of Berryman et al. (2011). Additionally, with precision and discrete sample measurement rates comparable to automated continuous-flow IRMS, this method further advances CRDS as an attractive alternative for trace gas isotope analysis.

2 Materials and methods

2.1 Analyser and sampling system

The CRDS instrument adapted for discrete sample measurement was a Picarro G2131-i isotopic-CO_2 gas analyser (Picarro Inc., Santa Clara, CA, USA). Detailed description of the operation and spectroscopy of the G2131-i and predecessor units

can be found in Dickinson et al. (2017), Hoffnagle (2015), Rella (2010a, 2010b, 2010c), and Wahl et al. (2006). In brief, sample air is circulated through a high-reflectivity optical cavity (35 cm^3) at an inlet flow rate of ca. 25 ml min^{-1} (NTP). Internal controls maintain the cavity at 318.150 ± 0.002 K and 18.67 ± 0.02 kPa. Spectroscopic ring-down time constants are measured across spectral bands of $^{12}C^{16}O_2$ and $^{13}C^{16}O_2$ to determine optical absorption peak heights, which are computed into $^{13}C/^{12}C$ isotope ratio and CO_2 mole fraction data (Hoffnagle, 2015). Spectral lines of $^{12}C^{1}H_4$ and $^{1}H_2{}^{16}O$ are also measured for correcting direct and indirect spectral interferences from H_2O and CH_4 on the CO_2 bands. The normal measurement range for the G2131-i is set at 380 to 2000 ppm xCO_2 and natural abundance to +5000 ‰ in $\delta^{13}C$-CO_2 (Picarro, 2011).

All measurements made by the G2131-i are continually recorded at a rate of ca. 0.8 Hz; specific data must be extracted from log files for further treatment. Although discrete sample measurement is thus possible without special provision – by inletting the G2131-i with 200 to 300 ml of sample from a gasbag or chamber and retrieving the relevant data (Picarro, 2012) – such procedure is time inefficient and prone to errors from operator inconsistency. Furthermore, in many research settings it is impractical or impossible to gather such large samples (e.g. headspace chamber analyses). By instead applying a controlled procedure for inletting smaller volumes and software to automatically process the raw data in real-time, a more feasible method of discrete sample measurement was created.

A schematic of our measurement set-up is shown in Fig. 1. The system was simple in construction and concept: hermetic sample collection and delivery was achieved by high-quality gas-tight syringe with push-button valve and Luer lock fitting (50 ml, SGE Analytical Sci., Australia). A low permeability multi-layer foil gasbag (27 L Plastigas, Linde AG, Germany) functioned as a reservoir for a standard reference air, which was analysed between individual samples so as to give a 'baseline' for accurate data delineation. The large, non-pressurised volume of the reservoir meant pressure induced mixing and back-flow risks were excluded, and allowed prolonged operation before refilling (>15 h). Gas-proof fluorinated-ethylene-propylene (FEP) tubing (Rotilabo, Carl Roth GmbH, Germany), Luer lock fittings, and Luer lock 3-way valves completed the set-up. All permanent tube fittings and joins were adhered with Loctite 406/770 (Henkel AG, Germany) to ensure robustness and prevent leakage. The FEP tubing between the syringe sample inlet point and the CRDS inlet port (Fig. 1) was minimised (⅛″ OD × 44 cm, connected to the ¼″ CRDS inlet port with reducing ferrule) to decrease mixing and lag time between sample delivery and measurement.

2.2 Sample measurement

The G2131-i and discrete sample measurement system were installed in an environmentally controlled laboratory (20 °C) to ensure stable operation. Syringed sample measurement was performed as follows: After instrument start-up and commencement of normal function, reference air measurement was initiated to establish stable baselines of xCO_2 and $\delta^{13}C$-CO_2. When a sample was ready for analysis, the syringe was connected to the sample inlet point (Fig. 1), and the 3-way

valve manually actuated to stop the flow of reference air and supply the sample directly to the analyser. Upon opening the syringe valve the gas sample was drawn into the G2131-i, causing steady, unassisted collapse of the syringe plunger. Sample evacuation was completed in ca. 2.5 min, after which the sample inlet point valve was immediately reset and reference air intake resumed. Once CO_2 and $\delta^{13}C$-CO_2 readings had returned to initial baseline levels (thereby safeguarding against sample-to-sample carryover), the process was repeated for the next sample. In this way, reference air readings were punctuated by syringe samples to create 'peaks' in the raw data output with a sample-to-sample time of ca. 5 min (Fig. 2). The gas aliquot size for all measurements was nominally 50 ml NTP. (Analysis of smaller amounts may be possible but 50 ml was assessed as a minimum for reliable operation. Samples larger than 50 ml would be easily handled, although adjustment of peak truncation parameters and re-calibration may be necessary for accurate performance – see below and Sect. 2.3.)

To achieve unambiguous sample peak identification, distinction in CO_2 was required between reference air and sample. In practice this meant a relative change of ca. 2 % in xCO_2 or ca. 5 ‰ in $\delta^{13}C$-CO_2. However, very large differences resulted in slower sample turnover (see Sect. 3.1). Best throughput was obtained using reference air that was similar to samples in xCO_2 but contrasting in $\delta^{13}C$-CO_2 (e.g. 15 ‰ difference). In this work, dry standard air with 496 ppm xCO_2 and -36.1 ‰ $\delta^{13}C$-CO_2 was used as the reference for all formal measurements (NA1, Table 1).

While sample measurement was performed manually (i.e. syringe connection and disconnection, valve operation etc.), to ensure method consistency we composed a custom computer software script to manage the process in real-time (script available in the Supplement). Running through the built-in 'Coordinator' software program of the G2131-i, our script prompted the user for correct timing of sample introduction, detected and extracted sample peak data, monitored reference air values, filtered problem measures, and recorded measurement results. The software script isolated individual samples from the CRDS data-stream by using specific events and timings in the measurement process as cues (e.g. a basic peak recognition algorithm; Fig. 3a). Prior to introduction of a sample, a reference air baseline was recorded for 30 s and averaged. Sample detection (trigger) then occurred when xCO_2 or $\delta^{13}C$-CO_2 values deviated from the baseline beyond a fixed threshold (default: 0.5 % of xCO_2 or 2 ‰ in $\delta^{13}C$-CO_2). The sample end (detrigger) was detected when measures returned halfway to baseline values (Fig. 3b). By truncating the sample peak data +80 s from the trigger and -29 s from the detrigger, ca. 30 s of representative measurement data was obtained for each sample (Fig. 3a). Upon completion of a sample measurement, the script computed means and standard deviations (SDs) of all data elements reported by the G2131-i (i.e. xH_2O and xCH_4 values together with xCO_2 and $\delta^{13}C$-CO_2). These statistics were compiled along with corresponding baseline measures, timestamped, assigned sample descriptors, and then outputted into a concise results file (see example in the Supplement). After each detrigger event the software monitored CRDS readings for return to initial reference air baseline values before directing the operator to proceed with the next sample.

In addition to the G2131-i analyser, our method was successfully trialled on a sister CRDS instrument (Picarro G2201-i). The G2201-i differs from the G2131-i only in additionally measuring $^{13}C^{1}H_4$ to give $\delta^{13}C\text{-}CH_4$ data (Picarro, 2015). To assist method adoption, we supply software scripts customised for each instrument (Supplement). The scripts include provision for user-adjustment of peak identification and truncation parameters to suit individual set-ups. A short video recording of the system and measurement demonstration is also available (https://youtu.be/jqVFUO-EuCk).

2.3 Measurement calibration

Conventional CRDS trace gas measurements are affected by signal noise, gradual instrument drift, and any unaddressed interferences or perturbations in the underlying spectroscopy (Vogel et al., 2013). Calibration strategies exist to counter both drift and spectral errors while random noise ultimately limits instrument precision (Friedrichs et al., 2010; Wen et al., 2013). In the present case of short discrete sample measures however, there was additional inaccuracy stemming from the nature of sample gas delivery into the CRDS analyser.

As discussed in studies by Gkinis et al. (2011) and Stowasser et al. (2012), stepwise changes to the inlet gas composition (as occur with discrete samples) do not give rise to correspondingly abrupt jumps in CRDS measurements, and instead result in sigmoid-shaped steps in the data (Fig. 3b). These smoothed transitions are the combined result of (i) the rate of gas replenishment in the optical cavity (Stowasser et al., 2014), (ii) partial mixing (turbulence and diffusion) of gas compositions downstream of the sample inlet (Gkinis et al., 2011), and (iii) molecular sorption and desorption on internal surfaces of the cavity and inlet tubes (Friedrichs et al., 2010). Although ‘response times’ of CRDS instruments typically range 1 to 3 min (Picarro, 2011; Sumner et al., 2011), the actual time required for an optical cavity to completely transition to a new gas composition can be substantially longer. In testing the G2131-i, we observed remnants of previous gases persisting with asymptotical decline for as long as 40 min following very large shifts in CO_2 composition (e.g. $|\Delta x CO_2|$ >10000 ppm or $|\Delta\delta^{13}C\text{-}CO_2|$ >5000 ‰). While the error caused by the residual gases may sometimes be relatively trivial, all measurements that occur prior to the cavity attaining equilibrium will experience these ‘memory effects’.

In our 50 ml syringe samples, memory effects were clearly present, as evidenced by the asymptotic curvature in the data peaks (Fig. 2). This meant that reported measures of syringe samples were biased towards reference air compared to ‘true’ values that would be eventually determined from measurements of indeterminately large sample volumes and monitoring for asymptotic closure. Other researchers have mitigated memory effects by evacuating the optical cavity before sample introduction (Berryman et al., 2011), or through several replicate measurements (Gupta et al., 2009; Leffler and Welker, 2013). Such solutions significantly reduce sample throughput however. In this work, we elected to post-correct for reference air carry-over by calibrating our method with bottled gas standards. More specifically, we compared discrete sample measurements of gas standards against measures of the same standards directly inlet to the G2131-i for prolonged periods (>1 h). Importantly, syringe measures were not calibrated directly against gravimetric values of the standards – here we were

only concerned with isolating and eliminating bias associated with the syringe sampling method and not with unaccounted inaccuracies or drift in instrument spectroscopy. This approach facilitates a more comprehensive examination of memory effects while also providing flexibility for method adaptation or applying additional error corrections for specific samples (e.g. adjusting for gas-matrix pressure broadening effects: Nara et al., 2012).

To this end, seven gravimetric gas standards were used as fixed source calibrants (0.05 to 2109 ppm xCO_2 and -27.3 to +21740 ‰ $\delta^{13}C$-CO_2(see Table 1; exact compositions detailed in Dickinson et al., 2017) . Using such a wide range of CO_2 compositions served to improve overall calibration accuracy as well as demonstrating reliability and applicability of method. Direct measurements were performed by inletting the bottled standards to the G2131-i for more than one hour to ensure the absence of memory effects before taking formal measures for 10 min (ca. 460 data points; averages reported in Table 1). Next, 50 ml syringe samples of the standards were taken directly from bottles (syringe was pre-flushed several times to preclude contamination) and measured as described in Sect. 2.2 (8 samples of each standard for 56 measures in total – dataset in the Supplement). Before further analysis, due to the high ^{13}C abundance in several gas standards, all CRDS reported CO_2 data were adjusted using the empirical correction described by Dickinson et al. (2017). (In testing CRDS performance with ^{13}C-enriched CO_2, Dickinson et al. identified minor but unaccounted spectroscopic cross-talk in $^{12}CO_2$ measurements at elevated levels of $^{13}CO_2$, as well as logical inconsistencies in the G2131-i data output. Their correction scheme was applied to the present data as a precaution to preclude any possibility that an underlying instrument error might obfuscate the memory effects in syringe sample measures.)

The relationship between syringe and bottle measurements was established by recognising that the data peaks generated by syringe samples could be approximated by generalised logistic curves (Fig. 3b; also Gkinis et al., 2011). From this, together with a constant aliquot size for all syringe measures, we were able to predict a simple linear scaling of syringe values:

$$syringe = base + (bottle - base)/\,K \qquad (1)$$

where *syringe* refers to the measurement value obtained for a syringe sample of a gas standard, *base* to the baseline measurement of reference air prior to sample introduction, *bottle* to the direct bottle measurement of the same standard, and K is a dimensionless empirical constant.

While all CO_2 data elements reported by the G2131-i exhibited reasonably similar sample peak geometry, the empirical constants for $^{12}CO_2$ and $^{13}CO_2$ were expected to differ due to (de)sorption and diffusion induced isotope fractionation during sample filling of the optical cavity. Further, theoretical gas mixing considerations entailed Eq. (1) would not consistently hold for $^{13}C/^{12}C$ isotope ratio data (R_{CO_2}) where a simultaneous change in total-xCO_2 also occurred. Consequently, only $x^{12}CO_2$ and $x^{13}CO_2$ data were explicitly calibrated, with R_{CO_2} being subsequently recalculated. (Moreover, only the dry mole fraction data of $^{12}CO_2$ and $^{13}CO_2$ were used due to the high likelihood of different transition equalisation rates for CO_2 and

H_2O. For explanation of dry and wet mole fraction data see: Hoffnagle, 2015; Rella, 2010a; Rella et al., 2013.) Accordingly, the following correction formulae were derived from Eq. (1):

$$x^{12}\mathrm{CO_2}(\mathrm{corrected}) = x^{12}\mathrm{CO_2}(\mathrm{base}) + [x^{12}\mathrm{CO_2}(\mathrm{syringe}) - x^{12}\mathrm{CO_2}(\mathrm{base})] \cdot K_{\mathrm{C12}} \quad (2)$$

$$x^{13}\mathrm{CO_2}(\mathrm{corrected}) = x^{13}\mathrm{CO_2}(\mathrm{base}) + [x^{13}\mathrm{CO_2}(\mathrm{syringe}) - x^{13}\mathrm{CO_2}(\mathrm{base})] \cdot K_{\mathrm{C13}} \quad (3)$$

Total-$x\mathrm{CO_2}$, $R_{\mathrm{CO_2}}$, and $\delta^{13}\mathrm{C\text{-}CO_2}$ data were then determined from the resulting corrected values of $x^{12}\mathrm{CO_2}$ and $x^{13}\mathrm{CO_2}$:

$$x\mathrm{CO_2} = x^{12}\mathrm{CO_2}(\mathrm{corrected}) + x^{13}\mathrm{CO_2}(\mathrm{corrected}) \quad (4)$$

$$R_{\mathrm{CO_2}} = \frac{x^{13}\mathrm{CO_2}(\mathrm{corrected})}{x^{12}\mathrm{CO_2}(\mathrm{corrected})} \quad (5)$$

$$\delta^{13}\mathrm{C\text{-}CO_2} = \left[\left(\frac{R_{\mathrm{CO_2}}}{R_{\mathrm{VPDB}}}\right) - 1\right] \cdot 1000\ ‰ \quad (6)$$

The correction constants, K_{C12} and K_{C13}, were found through weighted least squares analysis (WLS) of Eqs. (2) and (3) with syringe and bottle measurements of gas standards as input data (i.e. reverse regression of Eq. 1; bottle measures substituting for the left-hand-sides of Eqs. 2 and 3). To increase statistical power, $R_{\mathrm{CO_2}}$ and total-$x\mathrm{CO_2}$ data from bottle measurements were also incorporated into the analysis with Eqs. (4) and (5), thereby forming an extended optimisation problem (n = 216). In a similar vein to the WLS approach used by both Dickinson et al. (2017) and Stowasser et al. (2014) for calibrating CRDS measures, residuals weights were taken as the reciprocals of the individual summed variances resulting from the SDs of each syringe sample and bottle measurement (see Supplement and Table 1). The WLS solution was determined in R (version 3.2.1; R Core Team, 2015) by general purpose optimisation using the L-BFGS-B algorithm (Zhu et al., 1997) to yield the best-fit correction constants for all available CO_2 mole fraction and $^{13}C/^{12}C$ isotope ratio data.

2.4 Precision and consistency tests

CRDS precision is generally assessed by the variability in repeated measurements of a homogenous gas source (e.g. the SD of multiple 5 min analyses; Vogel et al., 2013; Wang et al., 2013). However, the internal variation in individual measurements can also be used to gauge analytic resolution (e.g. the SD of data contained in a 10 min measure – as with the bottle measurements in Sect. 2.3, also Pang et al., 2016 and Stowasser et al., 2014). For our case of 50 ml syringe samples, precision was quantified in both ways: The SD of the 30 s of CRDS data composing each individual sample (intra-sample SD, see Sect. 2.2), and as the statistical dispersion of replicate samples (inter-sample SD).

We tested method precision by repeated measurements of a systematic set of gas mixtures that spanned the normal operational CO_2 range of the G2131-i. Using gas standards as blending sources (Table 1; Dickinson et al., 2017), 20 unique mixes with varied CO_2 mole fractions (ca. 300, 600, 1000, 1500, 2000 ppm) and $\delta^{13}\mathrm{C\text{-}CO_2}$ values (ca. -30, +800, +1750, +2700, +3600 ‰) were prepared into multi-layer foil gasbags (1000 ml Supel Inert, Sigma-Alrich Corp., St. Louis, MO, USA). (The set of mixtures formed an orthogonal array of cross combinations of $x\mathrm{CO_2}$ and $\delta^{13}\mathrm{C\text{-}CO_2}$ meaning any

interdependency in precision could be identified.) Each mix was sampled and measured with the syringe method three times in succession, and results analysed for inter- and intra-measurement variation.

Long-term consistency and reliability of our syringe method was assessed by periodic analysis of a standard air (NA2, Table 1) during the course of 9 months of routine instrument use. More than 200 measurements were conducted and results examined for precision and drift.

3 Results and discussion

3.1 System operation

Though somewhat labour intensive and requiring continual operator attention, the syringe sample measurement process was uncomplicated, reliable, and economical. Sample handling and CRDS operation was non-specialist in comparison to conventional IRMS. The method was flexible to CO_2 composition, successfully handling samples <0.1 to >20000 ppm xCO_2 and -100 to +30000 ‰ $\delta^{13}C\text{-}CO_2$. The only significant methodological constraint observed was a reduction in sample turnover rate for compositions greater than either 3000 ppm xCO_2 or +4000 ‰ $\delta^{13}C\text{-}CO_2$. This was because post-sample reference air measures took longer to return to pre-sample baselines due to memory effects, thereby extending the inter-sample period. Keeping CO_2 levels within G2131-i specifications resulted in a throughput of ca. 10 samples h^{-1}. Best measurement rates of 12 to 13 samples h^{-1} occurred when sample CO_2 compositions neighboured the reference air (e.g. within ca. 100 ppm xCO_2 and ca. 20 ‰ $\delta^{13}C\text{-}CO_2$ of reference). These throughput rates are at least a 2-fold improvement over both the method of Berryman et al. (2011) and specialty peripheral devices (Picarro, 2013).

Following initial development, the syringe method was incorporated into our general laboratory practices and during the first year of implementation more than 10000 samples were measured. Despite intense instrument usage, we noticed no changes or adverse impacts on G2131-i function, although increased external pressure variations caused by frequent syringe evacuations may conceivably reduce mechanical lifetimes of optical cavity pressure control valves. Failures occurred in ca. 1 % of measurements, principally due to operator mistakes, but occasionally because of leakage in sample inlet valve, syringe fault, or complications from the peak identification algorithm for samples very similar to the reference air (see Sect. 2.2). Very rarely, minor instabilities in reference air readings caused false peak detections and baseline return problems, but such instances were usually identified by the software script and internally resolved.

Durability of the gas-tight syringes used for sample delivery was excellent, although regular monitoring and maintenance was important to ensure smooth sample evacuation during the measurement process. Excessive plunger friction led to significant ‘jumpiness’ in syringe collapse, which manifested as small pressure fluctuations to the optical cavity and increased measurement noise (evidenced by larger reported SDs). Careful cleaning and exact silicone lubrication was carried

out every few hundred samples to ensure uniform plunger operation and prolongation of syringe life. Syringe push-button and sample inlet point valves also required periodic attention and were replaced as necessary to pre-empt leaks and breakages.

3.2 Correction of memory effects

From rearranging Eq. (1), the discrepancy between syringe and bottle measurements (syringe bias) was predicted to be proportional to the difference of the syringe value and reference air baseline (sample peak height):

$$(syringe - bottle) = (syringe - base) \cdot (1 - K) \quad (7)$$

Comparing the actual syringe sample and bottle measurements of gas standards, we observed systematic memory effect bias that was indeed consistent with this postulated relationship (Fig. 4). WLS across all CO_2 data yielded estimates of 1.00341 for K_{C12} and 1.00440 for K_{C13}, with a coefficient of determination (r^2) of 0.84 (weighted residuals) for the complete correction model. Standard errors for K_{C12} and K_{C13} estimates were respectively 0.00017 and 0.00014 (see confidence intervals in Fig. 4). The Pearson's correlation coefficient between K_{C12} and K_{C13} estimates was 0.26. The observed divergence in correction constants for $^{12}CO_2$ and $^{13}CO_2$ was statistically significant (t-test: $P < 0.0001$) with a larger memory effect present in $^{13}CO_2$ measurements. This result corroborates the expectation of isotope fractionation occurring during gas equalisation in the CRDS optical cavity, putatively due to surface (de)sorption and diffusion phenomena.

Having determined K_{C12} and K_{C13}, syringe CO_2 measurements can be adjusted for bias with Eqs. (2)–(6). Accuracy of these corrections is very good: The standard errors on K_{C12} and K_{C13} add uncertainty to $x$$CO_2$ and δ^{13}C-CO_2 data of less than 0.02 % of the difference between the sample and baseline values. For atmospheric samples, this additional source of error is entirely negligible compared to the uncertainty deriving from measurement precision and gas standard analytical accuracy.

While the correction coefficients (K_{C12} and K_{C13}) found in this work are unique to our sampling equipment and G2131-i analyser, the equivalent calibration may be easily performed on replica set-ups. We provide a generic spreadsheet to post-correct syringe sample CO_2 data for any values of K_{C12} and K_{C13}, and a template for simultaneously applying the syringe correction with the spectroscopic calibration strategy of Dickinson et al. (2017) for ^{13}C-enriched samples (Supplement). Although our work only addresses memory effect bias in CO_2 data, we are confident the same strategy (Eq. 1) is straightforwardly applicable to other gas species (and isotopes) that can be similarly analysed by syringed samples and CRDS (e.g. CH_4, H_2O, N_2O).

3.3 Measurement precision and consistency

Replicate tests provided a practical account of precision afforded by our discrete sample measurement system. Figure 5 shows inter- and intra-sample SDs and relative SDs for $^{12}CO_2$ and $^{13}CO_2$ mole fraction data (complete dataset in the

Supplement). The SDs of both species were generally proportional to their measured values and unaffected by $\delta^{13}C\text{-}CO_2$ level (i.e. precision in $^{12}CO_2$ and $^{13}CO_2$ measurements were mutually independent). Relative SDs for both isotopolouges remained near constant at ≤0.05 % across the tested ranges however (Fig. 5c, d). Notably, the majority of intra-sample SDs for both $x^{12}CO_2$ and $x^{13}CO_2$ data were found to be in general agreement with counterpart inter-sample SDs (see trendlines in Fig. 5). This means that the SDs reported by our software script for $^{12}CO_2$ and $^{13}CO_2$ mole fractions in individual syringe sample measures will reasonably approximate the expected precision for replicated measurements of those samples.

On the other hand, inter- and intra-sample SDs in $^{13}C/^{12}C$ isotope ratio data were dependent on the $\delta^{13}C\text{-}CO_2$ level and CO_2 mole fraction, increasing with higher $\delta^{13}C\text{-}CO_2$ and lower xCO_2 (see Fig. S1a, b in the Supplement). The relative SDs of isotope ratio measurements were unaffected by $\delta^{13}C\text{-}CO_2$ level but steadily decreased with increasing xCO_2 – declining from between 0.07 and 0.04 % at 300 ppm xCO_2 to between 0.03 and 0.015 % at 2000 ppm (Fig. S1d). One exception was at natural abundance isotope ratios ($\delta^{13}C\text{-}CO_2 \approx$ -30 ‰) where inter-sample relative SDs of R_{CO_2} were steady at ca. 0.015 % (i.e. 0.15 ‰) across the tested xCO_2 range (Fig. S1b). Somewhat opposing CO_2 mole fraction data, intra-sample SDs of isotope ratio data were almost always greater than corresponding inter-sample SDs, which largely reflects the summation of variance from the $^{12}CO_2$ and $^{13}CO_2$ spectral measurements used to produce the $^{13}C/^{12}C$ ratios. Nevertheless, as with $^{12}CO_2$ and $^{13}CO_2$, the SD reported for $\delta^{13}C\text{-}CO_2$ in individual syringe sample measures may be used as a conservative proxy of $\delta^{13}C\text{-}CO_2$ replicate precision.

Consistency of the syringed sample method was established by long-term repeated analysis of a standard air (NA2, Table 1). Figure 6 shows $x^{12}CO_2$ and $\delta^{13}C\text{-}CO_2$ data from 200 measurements covering a 9-month period (dataset available in the Supplement). It is important to note that because these data were only adjusted for memory effects inherent to the discrete sample system (i.e. by Eqs. 2–6), they represent a simultaneous time-series test of instrument stability and methodological constancy. The measures averaged 1024.18 ppm in $x^{12}CO_2$ and -27.35 ‰ in $\delta^{13}C\text{-}CO_2$ with respective SDs of 0.50 ppm and 0.33 ‰. The latter SD is larger than the inter-sample SD found in replicate measure testing (0.15 ‰, see above), likely indicating the presence of instrument drift in the data in addition to random errors of repeated syringe sampling. While the separate components of variance cannot be resolved here, moving-means (red lines in Fig. 6) show neither a sustained trend nor method discontinuity, and imply that reasonable measurement accuracy is possible under typical laboratory practices without perpetual calibration against gas standards (compare syringe sample measures against the direct bottle measurement of NA2; Fig. 6), corroborating the similar conclusion reached by Friedrichs et al. (2010). The mean of intra-sample SDs in the 200 measures was 0.42 ppm for $x^{12}CO_2$ and 0.35 ‰ for $\delta^{13}C\text{-}CO_2$, both corresponding well to the aforementioned SDs of all measurements and the intra-sample SDs in the replicate tests. This consistency further supports our proposition that a single syringe measure and its intra-sample SD can deliver a similar (although inherently less reliable) statistical estimate to one generated through multiple sample measurements, potentially making replicate CRDS analyses unnecessary in research contexts where statistical uncertainty is not a critical consideration.

In sum, despite the short CRDS analysis period for a syringe sample (ca. 30 s), and limited number of replicates in performance testing, achieved measurement precision was excellent. With our system and G2131-i analyser, replicate sample SDs of ≤0.05 % may be expected for $^{12}CO_2$ and $^{13}CO_2$ mole fraction data, while resolution in repeated $\delta^{13}C\text{-}CO_2$ measurements will be ca. 0.15 ‰ at natural ^{13}C abundance. Moreover, to a first approximation, similar precisions can be obtained from intra-sample SDs of single syringe sample measures. These results should be viewed tentatively if adapting our method to a different model of CRDS analyser however. Because observed measurement variation derives from both volatility in the discrete sampling method and noise inherent to the instrument, matching the precision reported here is unlikely with lower performance CRDS units. As a point of reference, when using the G2131-i for continuous analysis of a homogeneous source, the inter-sample SDs for sequential 30 s data segments are ca. 0.15 ‰ in $\delta^{13}C\text{-}CO_2$ and 0.01 % in both $x^{12}CO_2$ and $x^{13}CO_2$, while intra-sample SDs are respectively ca. 0.30 ‰ and 0.025 % (Dickinson et al., 2017; also manufacturer specifications: Picarro, 2011).

Comparing to other CRDS discrete sample methods, our results improve upon the 0.3 % (xCO_2) and 0.3 ‰ ($\delta^{13}C\text{-}CO_2$) precision attained by Berryman et al. (2011), although this is probably due to the enhanced spectroscopic sensitivity of the G2131-i relative to the older G1101-i analyser used in their study. Additionally, our method delivers precision in $\delta^{13}C\text{-}CO_2$ that is similar to both the Picarro SSIM2 discrete sample peripheral device (0.11 ‰; Picarro, 2013) and traditional continuous-flow IRMS (typically 0.1 ‰), which, by contrast, are single-purpose instruments that do not also report accurate CO_2 mole fraction measurements. And finally, although finer measurement resolution is possible with CRDS, the uncertainties deriving from the precision of our discrete sample measures will be, in many cases, no worse than the tolerances on gravimetric gas standards used for instrument calibrations (cf. Brewer et al., 2014; Dickinson et al., 2017). In such contexts, applying our method for isotopic and mole fraction analyses of trace gases should not result in significantly poorer absolute accuracy compared to other sampling techniques (i.e. uncertainties on gas standards, rather than measurement precision, may limit overall accuracy).

3.4 Potential applications

At present, isotope ratio analysis of fixed trace gas samples is usually accomplished by IRMS interfaced to autosampling GC systems. Such instruments require specialised user training and carry high consumable costs however. Similarly capable CRDS-based techniques can avoid both these limitations and represent an advance in stable isotope analysis. Although not suitable for all sample types (e.g. non-atmospheric compositions of background gases; Friedrichs et al., 2010), adapting the present generation of CRDS gas analysers for rapid discrete sample measurement has promising application in contexts where syringe or flask sampling is frequently performed – especially where accurate gas mole fraction data is also valuable – such as in ecosystem respiration and emission studies (cf. Zeeman et al., 2008), analysing dissolved gases in terrestrial waters (Hope et al., 1995; Loose et al., 2009), and certain instances of trapped air in ice-cores (e.g. Sowers et al., 2005).

A specific example where our method has immediate relevance is in measuring CO_2 respiration in soil microcosm headspace studies. To date, applying CRDS gas analysers to such research is mostly achieved through closed-loop recirculation (Christiansen et al., 2015; Ramlow and Cotrufo, 2017) or continuous analysis of open chamber systems (Bai et al., 2011; Jassal et al., 2016). Apart from cost and complexity, these solutions restrict the number of experiments that can be concurrently measured by a single instrument. Our system significantly eases this constraint however. For instance, assuming a sample turnover of 10 h^{-1} and conducting four syringed headspace measures per microcosm over the course of a 10 h workday, it is feasible to use one analyser for measuring daily respiration rates in 25 simultaneous experiments. Further, where CO_2 flux partitioning by isotopic analysis is undertaken, achieving sample measurement precision of ca. 0.05 % in xCO_2 and ca. 0.15 ‰ in $\delta^{13}C$-CO_2 means that the resulting uncertainties on efflux partitions will be comparable (if not smaller) to those in studies using infrared gas analysis and IRMS or IRMS alone (cf. Joos et al., 2008; Munksgaard et al., 2013).

The primary drawbacks of employing our method for isotopic-CO_2 measurement of discrete samples compared to an automated GC-IRMS system are (i) the larger sampling size, (ii) a more constrained operational xCO_2 range, and (iii) the necessity of near-continuous operator presence at the instrument. However, implementation of smaller volume CRDS optical cavities (8.5 cm^3) could dramatically decrease the required sample amount and allow even shorter measurement times (e.g. Stowasser et al., 2014), while dilution methods and calibration can expand the xCO_2 measurement range of CRDS. Similarly, methodological refinement to integrate automated syringe sampling and valve systems would curtail labour requirements.

4 Conclusions and outlook

Discrete sample analysis of trace gases by CRDS is possible through basic instrument adaptation. We have set forth a scheme for xCO_2 and $\delta^{13}C$-CO_2 determination of 50 ml syringed samples on a Picarro G2131-i isotopic-CO_2 analyser. With software to manage the measurement process and compute results data, our method offers substantially faster analysis of small gas volumes with equal or better precision than comparable set-ups. Memory effects present in syringe sample measurements can be accurately compensated by calibration against large-volume measures of gravimetric gas standards.

Although CRDS is gaining scientific acceptance for isotopic-CO_2 measurement, so far the technology has not seriously challenged IRMS in discrete gas sample analysis, despite lower running and capital costs, simpler operation, less measurement drift, and the added benefit of providing more accurate xCO_2 data concurrently with $\delta^{13}C$-CO_2. In achieving comparable precision and sample throughput to IRMS, our syringe sample method helps position CRDS as a tenable competitor for isotopic analysis of discrete samples.

The chief disadvantages of our process compared to IRMS for isotopic-CO_2 analysis are a narrower xCO_2 performance range, higher labour demands, and a comparatively large sample size (50 ml NTP). Method improvements towards automation may greatly ease user workload however, and the development of smaller optical cavities could reduce the sample gas needed for discrete analysis on future CRDS analysers as well as increasing sample throughput rates even further.

This system can be applied with any Picarro G2131-i or G2201-i CRDS analyser, though calibration and tuning of parameters in the software script may be necessary to account for variations in set-up, sample volume (and pressure), and reference air composition. Implementation on other CRDS instruments and conversion for measurements of other trace gases are anticipated with only minor software amendments.

Supplement items

- Fig. S1. Precision in syringe sample $^{13}C/^{12}C$ isotope ratio data
- Discrete sampling software scripts for Picarro G2131-i and G2201-i analysers
- Example_discrete_sample_data_output.csv
- Measurement_data.xlsx
- Templates for bias correction (2)

Acknowledgements.

We are grateful to our ISOFYS colleagues Stijn Vandevoorde, Hannes De Schepper, and Katja Van Nieuland for their assistance with instrument operation and numerous sample measurements. We also thank Lei Liu (CREAF-CSIC, Barcelona, Spain) for testing our method on a Picarro G2201-i CRDS unit and for providing feedback on method efficacy. Renato Winkler from Picarro Inc. aided this work with his useful advice on developing software scripts for the G2131-i analyser. Finally, we thank the associate editor and two anonymous referees whose comments helped refine this paper.

References

Albanito, F., McAllister, J. L., Cescatti, A., Smith, P., and Robinson, D.: Dual-chamber measurements of $\delta^{13}C$ of soil-respired CO_2 partitioned using a field-based three end-member model, Soil Biol. Biochem., 47, 106-115, 2012.

Bai, M., Köstler, M., Kunstmann, J., Wilske, B., Gattinger, A., Frede, H.-G., and Breuer, L.: Biodegradability screening of soil amendments through coupling of wavelength-scanned cavity ring-down spectroscopy to multiple dynamic chambers, Rapid Commun. Mass Spectrom., 25, 3683-3689, 2011.

Berryman, E. M., Marshall, J. D., Rahn, T., Cook, S. P., and Litvak, M.: Adaptation of continuous-flow cavity ring-down spectroscopy for batch analysis of $\delta^{13}C$ of CO_2 and comparison with isotope ratio mass spectrometry, Rapid Commun. Mass Spectrom., 25, 2355-2360, 2011.

Brewer, P. J., Brown, R. J., Miller, M. N., Miñarro, M. D., Murugan, A., Milton, M. J., and Rhoderick, G. C.: Preparation and Validation of Fully Synthetic Standard Gas Mixtures with Atmospheric Isotopic Composition for Global CO_2 and CH_4 Monitoring, Anal. Chem., 86, 1887-1893, 2014.

Christiansen, J. R., Outhwaite, J., and Smukler, S. M.: Comparison of CO_2, CH_4 and N_2O soil-atmosphere exchange measured in static chambers with cavity ring-down spectroscopy and gas chromatography, Agr. Forest. Meteorol., 211–212, 48-57, 2015.

Crosson, E. R.: A cavity ring-down analyzer for measuring atmospheric levels of methane, carbon dioxide, and water vapor, Appl. Phys. B, 92, 403-408, 2008.

Crosson, E. R., Ricci, K. N., Richman, B. A., Chilese, F. C., Owano, T. G., Provencal, R. A., Todd, M. W., Glasser, J., Kachanov, A. A., Paldus, B. A., Spence, T. G., and Zare, R. N.: Stable isotope ratios using cavity ring-down spectroscopy: Determination of $^{13}C/^{12}C$ for carbon dioxide in human breath, Anal. Chem., 74 , 2003-2007, 2002.

Dahnke, H., Kleine, D., Urban, W., Hering, P., and Mürtz, M.: Isotopic ratio measurement of methane in ambient air using mid-infrared cavity leak-out spectroscopy, Appl. Phys. B, 72, 121-125, 2001.

Dickinson, D., Bodé, S., and Boeckx, P.: Measuring ^{13}C-enriched CO_2 in air with a cavity ring-down spectroscopy gas analyser: Evaluation and calibration, Rapid Commun. Mass Spectrom., doi: 10.1002/rcm.7969, 2017.

Friedrichs, G., Bock, J., Temps, F., Fietzek, P., Körtzinger, A., and Wallace, D. W. R.: Toward continuous monitoring of seawater $^{13}CO_2/^{12}CO_2$ isotope ratio and pCO_2: Performance of cavity ringdown spectroscopy and gas matrix effects, Limnol. Oceanogr. Methods, 8, 539-551, 2010.

Gkinis, V., Popp, T. J., Blunier, T., Bigler, M., Schupbach, S., Kettner, E., and Johnsen, S. J.: Water isotopic ratios from a continuously melted ice core sample, Atmos. Meas. Tech., 4, 2531-2542, 2011.

Gupta, P., Noone, D., Galewsky, J., Sweeney, C., and Vaughn, B. H.: Demonstration of high-precision continuous measurements of water vapor isotopologues in laboratory and remote field deployments using wavelength-scanned cavity ring-down spectroscopy (WS-CRDS) technology, Rapid Commun. Mass Spectrom., 23, 2534-2542, 2009.

Hancock, G. and Orr-Ewing, A. J.: Applications of Cavity Ring-Down Spectroscopy in Atmospheric Chemistry. In: Cavity Ring-Down Spectroscopy, John Wiley & Sons, Ltd, 2010.

Hoffnagle, J.: Understanding the G2131-i isotopic carbon dioxide data log. Picarro Inc., Santa Clara, California, USA, 2015.

Hope, D., Dawson, J. J. C., Cresser, M. S., and Billett, M. F.: A method for measuring free CO_2 in upland streamwater using headspace analysis, J. Hydrol., 166, 1-14, 1995.

Jassal, R. S., Webster, C., Black, T. A., Hawthorne, I., and Johnson, M. S.: Simultaneous Measurements of Soil CO_2 and CH_4 Fluxes Using Laser Absorption Spectroscopy, Agric. Environ. Lett., 1, 2016.

Joos, O., Saurer, M., Heim, A., Hagedorn, F., Schmidt, M. W. I., and Siegwolf, R. T. W.: Can we use the CO_2 concentrations determined by continuous-flow isotope ratio mass spectrometry from small samples for the Keeling plot approach?, Rapid Commun. Mass Spectrom., 22, 4029-4034, 2008.

Kerstel, E. R. T., Iannone, R. Q., Chenevier, M., Kassi, S., Jost, H. J., and Romanini, D.: A water isotope (^{2}H, ^{17}O, and ^{18}O) spectrometer based on optical feedback cavity-enhanced absorption for in situ airborne applications, Appl. Phys. B, 85, 397-406, 2006.

Leffler, A. J. and Welker, J. M.: Long-term increases in snow pack elevate leaf N and photosynthesis in Salix arctica: responses to a snow fence experiment in the High Arctic of NW Greenland, Environ. Res. Lett., 8, 025023, 2013.

Loose, B., Stute, M., Alexander, P., and Smethie, W. M.: Design and deployment of a portable membrane equilibrator for sampling aqueous dissolved gases, Water Resour. Res., 45, 6, 2009.

McAlexander, W. I., Fellers, R., Owano, T. G., and Baer, D. S.: Carbon isotope analysis of discrete CO_2 samples ranging from 300 ppmv to 100% using cavity enhanced laser absorption, European Geophysical Union General Assembly, Vienna, Austria, 2010.

Midwood, A. J. and Millard, P.: Challenges in measuring the $\delta^{13}C$ of the soil surface CO_2 efflux, Rapid Commun. Mass Spectrom., 25, 232-242, 2011.

Midwood, A. J., Thornton, B., and Millard, P.: Measuring the ^{13}C content of soil-respired CO_2 using a novel open chamber system, Rapid Commun. Mass Spectrom., 22, 2073-2081, 2008.

Munksgaard, N. C., Davies, K., Wurster, C. M., Bass, A. M., and Bird, M. I.: Field-based cavity ring-down spectrometry of $\delta^{13}C$ in soil-respired CO_2, Isotopes Environ. Health Stud., 49, 232-242, 2013.

Mürtz, M. and Hering, P.: Cavity Ring-Down Spectroscopy for Medical Applications. In: Cavity Ring-Down Spectroscopy, John Wiley & Sons, Ltd, 2010.

Nara, H., Tanimoto, H., Tohjima, Y., Mukai, H., Nojiri, Y., Katsumata, K., and Rella, C. W.: Effect of air composition (N_2, O_2, Ar, and H_2O) on CO_2 and CH_4 measurement by wavelength-scanned cavity ring-down spectroscopy: calibration and measurement strategy, Atmos. Meas. Tech., 5, 2689-2701, 2012.

Pang, J., Wen, X., Sun, X., and Huang, K.: Intercomparison of two cavity ring-down spectroscopy analyzers for atmospheric $^{13}CO_2/^{12}CO_2$ measurement, Atmos. Meas. Tech., 9, 3879-3891, 2016.

Picarro: G2131-i Analyser for Isotopic CO_2 User's Guide. Picarro Inc., Santa Clara, California, USA, 2012.

Picarro: Picarro A0314 Small Sample Isotope Module 2. Picarro Inc., Santa Clara, California, USA, 2013.

Picarro: Picarro G2131-i $\delta^{13}C$ High-Precision Isotopic CO_2 CRDS Analyzer. Picarro Inc., Santa Clara, California, USA, 2011.

Picarro: Picarro G2201-i CRDS Analyzer for Isotopic Carbon in CO_2 and CH_4. Picarro Inc., Santa Clara, California, USA, 2015.

Picarro: WS-CRDS for Isotopes – Cost of Measurement Comparison with IRMS for Liquid Water. Picarro Inc., Sunnyvale, California, USA, 2009.

R Core Team: R: A Language Environment for Statistical Computing. R Foundation for Statistical Computing, Vienna, Austria, 2015.

Ramlow, M. and Cotrufo, M. F.: Woody biochar's greenhouse gas mitigation potential across fertilized and unfertilized agricultural soils and soil moisture regimes, GCB Bioenergy, doi: 10.1111/gcbb.12474, 2017.

Rella, C.: Accurate stable carbon isotope ratio measurements in humid gas streams using the Picarro $\delta^{13}CO_2$ G2101-i gas analyzer. Picarro Inc., Sunnyvale, California, USA, 2010a.

Rella, C.: Accurate stable carbon isotope ratio measurements with rapidly varying carbon dioxide concentrations using the Picarro $\delta^{13}CO_2$ G2101-i gas analyzer. Picarro Inc., Sunnyvale, California, USA, 2010b.

Rella, C.: Reduced drift, high accuracy stable carbon isotope ratio measurements using a reference gas with the Picarro $\delta^{13}CO_2$ G2101-i gas analyzer. Picarro Inc., Sunnyvale, California, USA, 2010c.

Rella, C. W., Chen, H., Andrews, A. E., Filges, A., Gerbig, C., Hatakka, J., Karion, A., Miles, N. L., Richardson, S. J., Steinbacher, M., Sweeney, C., Wastine, B., and Zellweger, C.: High accuracy measurements of dry mole fractions of carbon dioxide and methane in humid air, Atmos. Meas. Tech., 6, 837-860, 2013.

Sigrist, M. W., Bartlome, R., Marinov, D., Rey, J. M., Vogler, D. E., and Wächter, H.: Trace gas monitoring with infrared laser-based detection schemes, Appl. Phys. B, 90, 289-300, 2008.

Snell, H. S. K., Robinson, D., and Midwood, A. J.: Minimising methodological biases to improve the accuracy of partitioning soil respiration using natural abundance ^{13}C, Rapid Commun. Mass Spectrom., 28, 2341-2351, 2014.

Sowers, T., Bernard, S., Aballain, O., Chappellaz, J., Barnola, J. M., and Marik, T.: Records of the $\delta^{13}C$ of atmospheric CH_4 over the last 2 centuries as recorded in Antarctic snow and ice, Global Biogeochem. Cycles, 19, 14, 2005.

Stowasser, C., Buizert, C., Gkinis, V., Chappellaz, J., Schüpbach, S., Bigler, M., Faïn, X., Sperlich, P., Baumgartner, M., Schilt, A., and Blunier, T.: Continuous measurements of methane mixing ratios from ice cores, Atmos. Meas. Tech., 5, 999-1013, 2012.

Stowasser, C., Farinas, A. D., Ware, J., Wistisen, D. W., Rella, C., Wahl, E., Crosson, E., and Blunier, T.: A low-volume cavity ring-down spectrometer for sample-limited applications, Appl. Phys. B, 116, 255-270, 2014.

Sumner, A. L., Hanft, E., Dindal, A., and McKernan, J.: Isotopic Carbon Dioxide Analyzers For Carbon Sequestration Monitoring Picarro Cavity Ring-Down Spectroscopy Analyzer For Isotopic CO_2 - Model G1101-i, Battelle Memorial Institute, Environmental Technology Verification Report 600F11053, 2011.

Vogel, F. R., Huang, L., Ernst, D., Giroux, L., Racki, S., and Worthy, D. E. J.: Evaluation of a cavity ring-down spectrometer for in situ observations of $^{13}CO_2$, Atmos. Meas. Tech., 6, 301-308, 2013.

Wahl, E. H., Fidric, B., Rella, C. W., Koulikov, S., Kharlamov, B., Tan, S., Kachanov, A. A., Richman, B. A., Crosson, E. R., Paldus, B. A., Kalaskar, S., and Bowling, D. R.: Applications of cavity ring-down spectroscopy to high precision isotope ratio measurement of $^{13}C/^{12}C$ in carbon dioxide, Isotopes Environ. Health Stud., 42, 21-35, 2006.

Wang, C., Miller, G. P., and Winstead, C. B.: Cavity Ringdown Laser Absorption Spectroscopy. In: Encyclopedia of Analytical Chemistry, John Wiley & Sons, Ltd, 2008.

Wang, J. L., Jacobson, G., Rella, C. W., Chang, C. Y., Liu, I., Liu, W. T., Chew, C., Ou-Yang, C. F., Liao, W. C., and Chang, C. C.: Flask sample measurements for CO_2, CH_4 and CO using cavity ring-down spectrometry, Atmos. Meas. Tech. Discuss., 6, 7633-7657, 2013.

Wen, X. F., Meng, Y., Zhang, X. Y., Sun, X. M., and Lee, X.: Evaluating calibration strategies for isotope ratio infrared spectroscopy for atmospheric $^{13}CO_2$ / $^{12}CO_2$ measurement, Atmos. Meas. Tech., 6, 1491-1501, 2013.

Werner, R. A. and Brand, W. A.: Referencing strategies and techniques in stable isotope ratio analysis, Rapid Commun. Mass Spectrom., 15, 501-519, 2001.

Zeeman, M. J., Werner, R. A., Eugster, W., Siegwolf, R. T. W., Wehrle, G., Mohn, J., and Buchmann, N.: Optimization of automated gas sample collection and isotope ratio mass spectrometric analysis of $\delta^{13}C$ of CO_2 in air, Rapid Commun. Mass Spectrom., 22, 3883-3892, 2008.

Zhu, C., Byrd, R. H., Lu, P., and Nocedal, J.: Algorithm 778: L-BFGS-B: Fortran subroutines for large-scale bound-constrained optimization, ACM T. Math. Software, 23, 550-560, 1997.

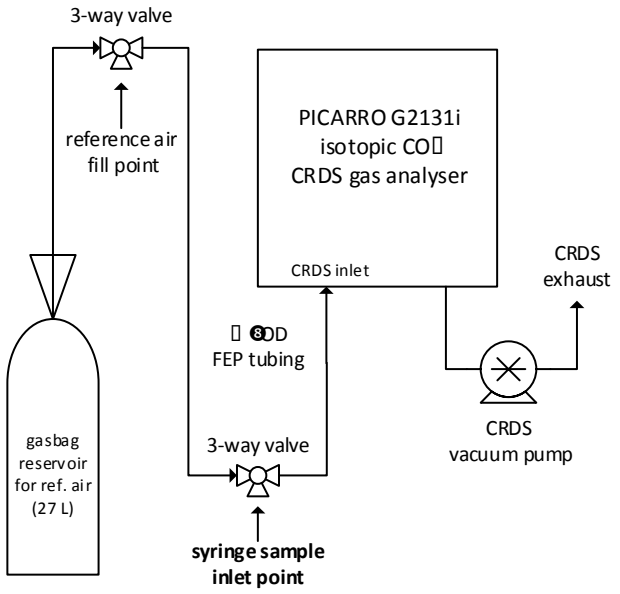

Figure 1: Schematic diagram of the discrete gas sample measurement system coupled to the isotopic-CO_2 CRDS analyser.

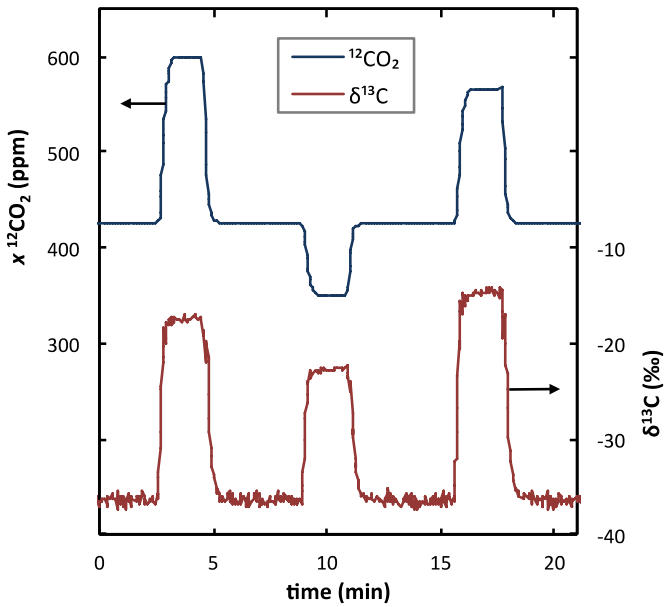

Figure 2: Example CRDS data feed for syringe samples. Reference air measurements (ca. 425 ppm $x^{12}CO_2$ and -37 ‰ $\delta^{13}C$-CO_2) are interrupted by successive samples to form consistently identifiable peaks in the data.

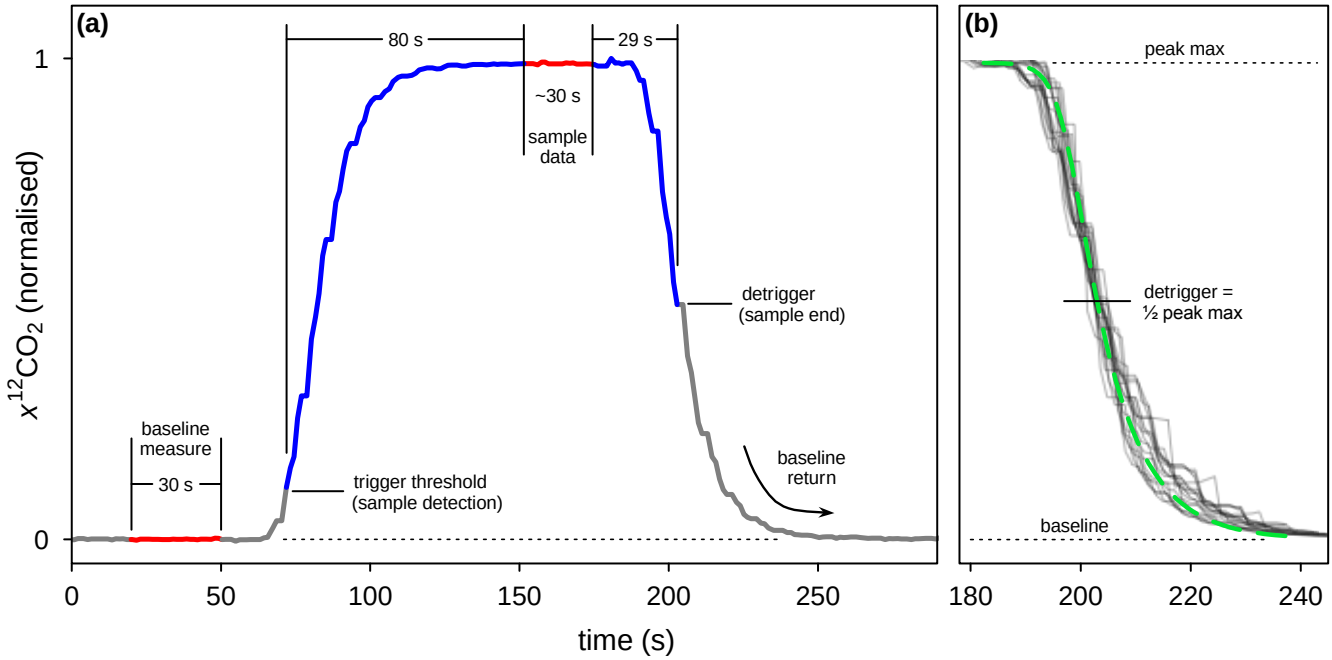

Figure 3: (a) Example of raw G2131-i measurement data and breakdown of events during analysis of a 50 ml syringe sample. Blue segments are truncated from the sample peak by our software script while red segments are the extracted measurement data. All timings and thresholds are user-customisable in the software for variation in sample size and equipment. (b) The most reliable sample end time (detrigger) was established as the point when measures returned to half the difference between peak-maximum (or minimum in the case of samples with lower xCO₂ than reference air) and the baseline value. Grey lines are amplitude-normalised tailing segments from 23 test samples widely varying in $x^{12}CO_2$. The broken green curve denotes a generalised logistic function fit to these test data by non-linear least squares optimisation. Solving the fitted function determined that 29 ± 2 s elapsed between peak-maximum and half-maximum irrespective of sample composition.

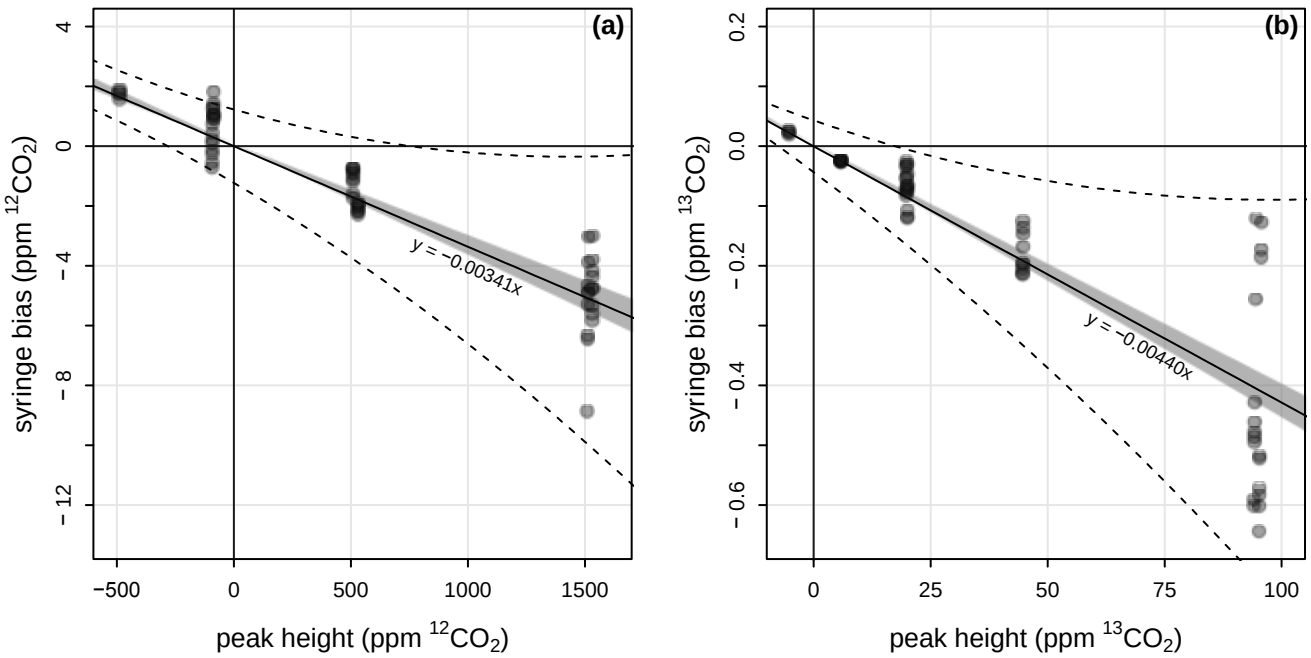

Figure 4: Discrepancies between syringe sample and direct bottle measurements (syringe bias) of gas standards as a function of the syringe sample peak height (Eq. 7) for (a) $x^{12}CO_2$ and (b) $x^{13}CO_2$. The WLS fitted linear models (see Sect. 2.3) are overlaid for comparison (solid lines; slopes = 1-*K*, Eq. 7), with 95 % confidence intervals (shaded) and 95 % prediction intervals (dashed lines) as determined from the standard error estimates of K_{C12} and K_{C13} (Sect. 3.2).

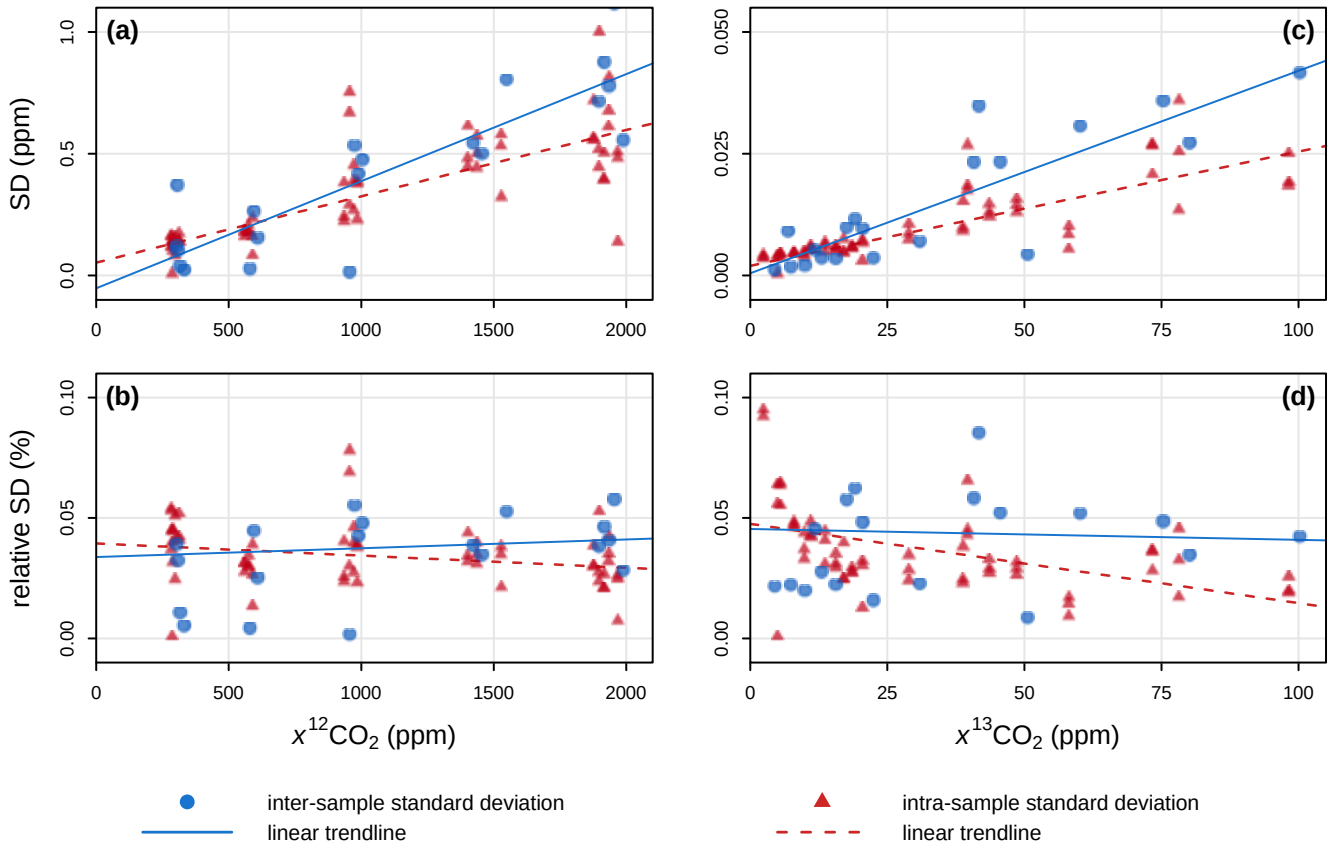

Figure 5: Precision in syringe sample data for $x^{12}CO_2$ (left: a, b) and $x^{13}CO_2$ (right: c, d) as quantified by standard deviations (top: a, c) and relative standard deviations (bottom: b, d) for individual measures (red) and replicate measurements (blue).

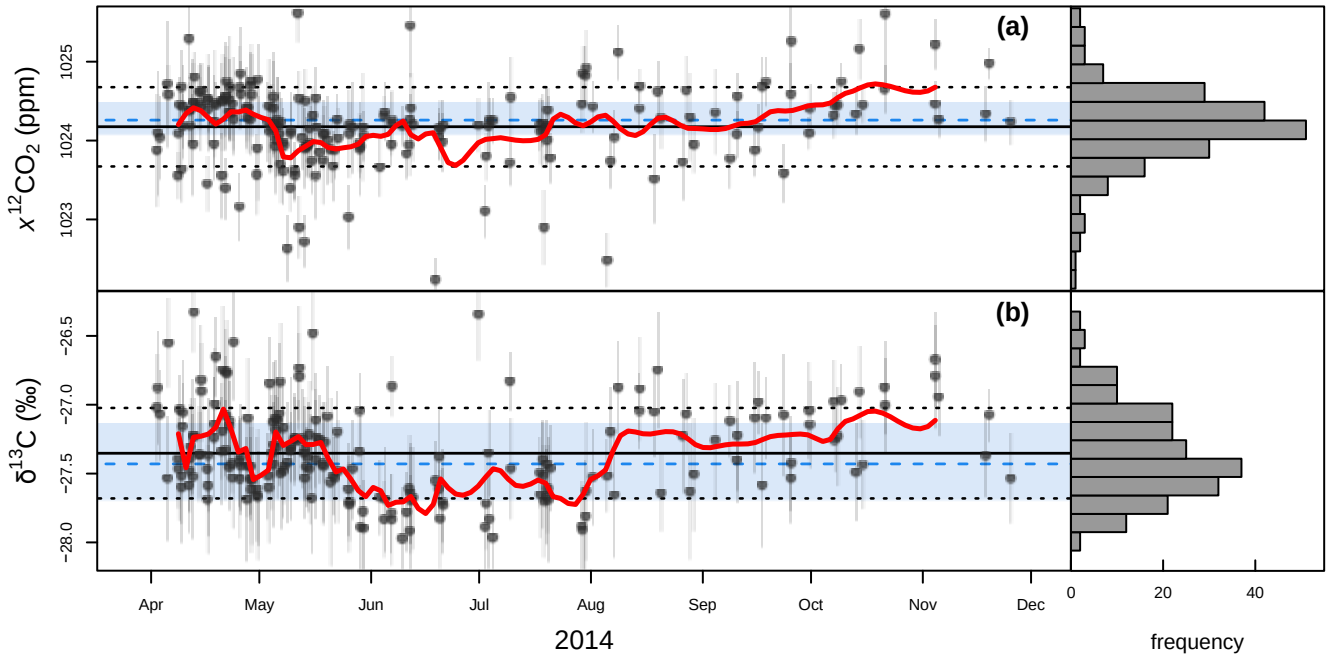

Figure 6: Repeated syringe sample measurements in (a) $x^{12}CO_2$ and (b) $\delta^{13}C$-CO_2 of standard gas NA2 (Table 1) over a 9-month period (n = 200). Error bars denote ±1 intra-sample SD of each individual measure. Grand means are the solid black horizontal lines with dotted lines indicating ±1 SD of all measurements. 10-sample moving averages are shown in red. Histograms inset right depict cumulative distributions of syringe measures. Blue dashed lines indicate the direct bottle measurement of NA2 with blue shaded areas covering ±1 SD of the bottle measure.

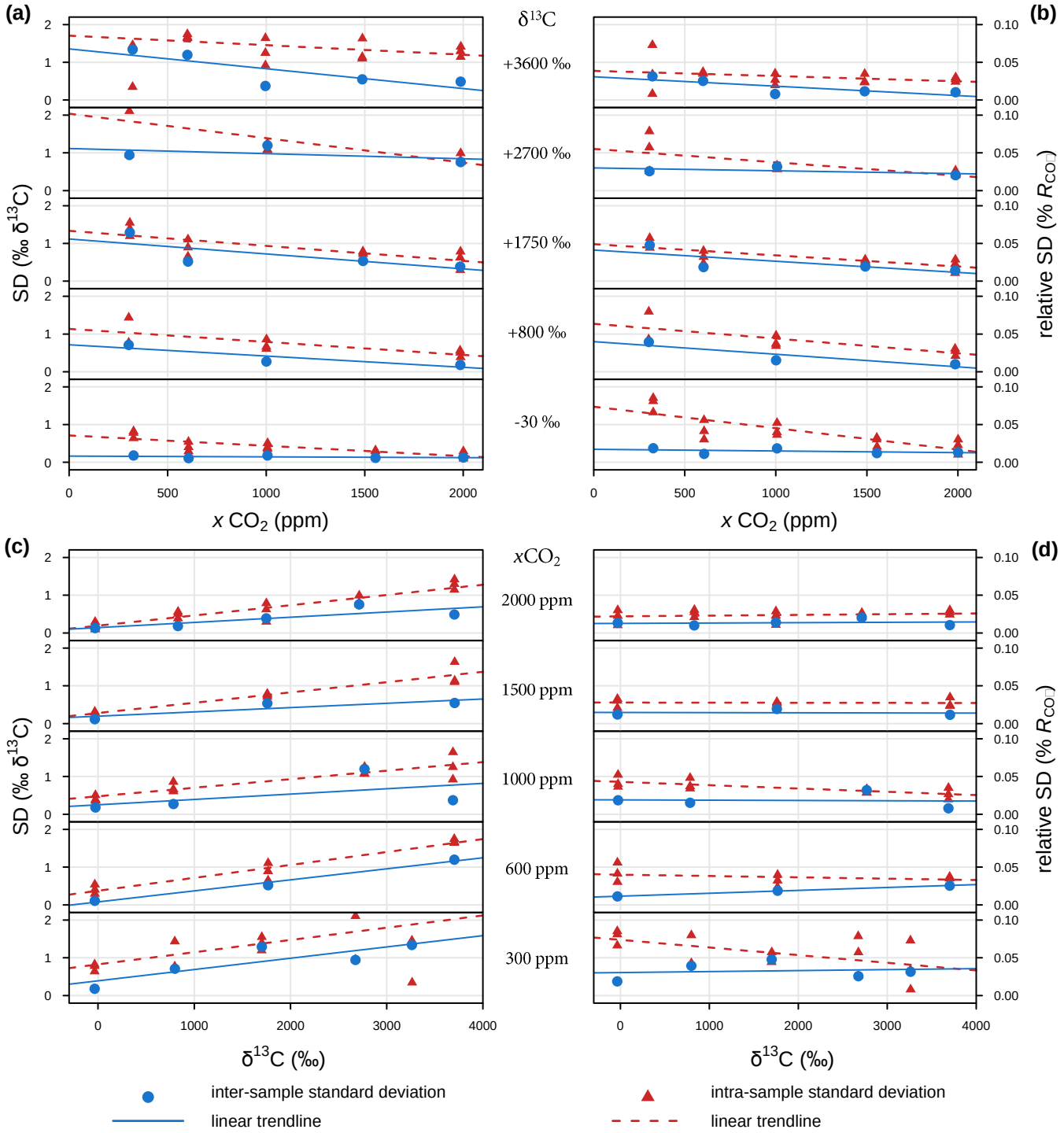

Figure S1: Precision in syringe sample $^{13}C/^{12}C$ isotope ratio data ($\delta^{13}C$-CO_2, R_{CO_2}) for individual measures (red) and replicate measurements (blue). (a) Standard deviations and (b) relative standard deviations as a function of total-CO_2 mole fraction and grouped by $\delta^{13}C$-CO_2. (c) Standard deviations and (d) relative standard deviations as a function of $\delta^{13}C$-CO_2 and grouped by total-*x*CO_2.

Standard ID	$x^{12}CO_2$ (ppm)	$x^{13}CO_2$ (ppm)	xCO_2 (ppm)	R_{CO_2} ($^{13}CO_2/^{12}CO_2$)*	$\delta^{13}C$-CO_2 (‰)**
NA1 (Ref. air)	490.55 (0.13)	5.286 (0.004)	495.84 (0.13)	1.0776 (0.0006)	-36.14 (0.57)
NA2	1024.26 (0.21)	11.137 (0.004)	1035.39 (0.21)	1.0874 (0.0003)	-27.43 (0.28)
ZERO	0.05 (0.04)	0.004 (0.004)	0.05 (0.04)	-	-
HE1	2028.98 (0.47)	25.528 (0.007)	2054.51 (0.47)	1.2582 (0.0004)	+125.35 (0.34)
HE2	2009.15 (0.53)	100.11 (0.02)	2109.26 (0.53)	4.983 (0.001)	+3456.9 (1.1)
TT	1002.18 (0.22)	50.216 (0.008)	1052.40 (0.22)	5.011 (0.001)	+3481.7 (1.1)
LE1	402.24 (0.11)	25.249 (0.005)	427.49 (0.11)	6.277 (0.002)	+4614.5 (1.7)
LE2	398.21 (0.16)	101.24 (0.01)	499.45 (0.16)	25.42 (0.01)	+21739 (9)

* R_{CO_2} data are scaled by 10^2 for ease of comprehension.

** $\delta^{13}C$-CO_2 values are reported against VPDB (Werner and Brand, 2001).

Table 1: Bottle measurement data of the standard air used as baseline for syringe sample measures (NA1) and the gas standards used in method calibration (NA2 through LE2). Values are the averages (SDs in parentheses) of 10 min measurements taken for each standard directly inlet to the CRDS analyser (see Sect. 2.3). Data have been post-corrected as per the calibration of Dickinson et al. (2017).